Study on Control Strategy of the New Type Hybrid Engraving Robot

Jiman Luo
School of Traffic and Mechanical Engineering, Shenyang Jianzhu University
Shenyang Jianzhu University, 9 Hunnan East RD, Shenyang, China
Syljm2004@163.com
Mingshan Zhang
School of Traffic and Mechanical Engineering, Shenyang Jianzhu University
Shenyang Jianzhu University, 9 Hunnan East RD, Shenyang, China
zms709370759@163.com
Qiaozhi Lin
School of Traffic and Mechanical Engineering, Shenyang Jianzhu University
Shenyang Jianzhu University, 9 Hunnan East RD, Shenyang, China
13709824171@163.com
Xiaowei Sun
School of Traffic and Mechanical Engineering, Shenyang Jianzhu University
Shenyang Jianzhu University, 9 Hunnan East RD, Shenyang, China
sunxiaowei989@163.com
Yuzhen An
School of Traffic and Mechanical Engineering, Shenyang Jianzhu University
Shenyang Jianzhu University, 9 Hunnan East RD, Shenyang, China
anyuzhen1987@163.com

Abstract

The new type hybrid engraving robot consists of a parallel working head and a machine body. It can realize 5 degrees of freedom (DOF) movement. The motion control of the parallel engraving working head is very difficult in the control of this robot. To deal with this problem, kinematic model of the new type engraving robot is developed firstly in this paper. The positive and inverse kinematic solutions of the model are calculated. Secondly, three control strategies are presented for this new type engraving robot. These include PD control, PD control with gravity compensation and the computed torque algorithm. Finally, mathematical models of these three algorithms are constructed by using Matlab\simulink software. The advantages and disadvantages of the algorithms are then discussed. It is found that computed torque algorithm is superior among the three for the position control of this new robot and the anti-jamming ability of this algorithm is very good. Therefore, a computed torque algorithm is adopted as the control strategy for the new type engraving rotor. Importantly, this control strategy is verified by experiment on the actual robot with the results comparing favourably with the simulated one.

Key words: hybrid engraving robot; engraving parallel working head; PD control algorithm; PD algorithm with gravity compensation; computed torque algorithm; Matlab\Simulink

1 Introduction

Research of hybrid engraving robots is currently very popular. A lot of domestic and foreign scholars present efforts on this topic. For example, [Bruno Monsarrat et al,2003] studied on workspace analysis and optimal design of a 3-leg 6-DOF parallel platform mechanism. For another example, [Joon Woo Kim et al, 2007] studied on stiffness analysis and design of a 3-DOF parallel robot with one constraining leg. Moreover, there are many other literatures in this research area, such as [Nicolas Lauzier et al, 2010; Chi Hyo Kim et al, 2007; Fabrizio Patan è and Paolo Cappa, 2011; Binbin Peng et al, 2010].

The new type of hybrid engraving robot can achieve three-dimensinal sculpture, three-dimensional milling, processing molding and other functions. It can be used for processing different materials such as wood, plastics, paraffin and so on. The new hybrid robot is composed of a gantry machine body and a parallel working head, which can realize 5-DOF's of movement. Figure 1 shows a physical model of hybrid robot and figure 2 illustrates a 3-D model of hybrid robot. The gantry machine body 2 can move in the direction along X axis and Y axis. The moving in X axis is implemented by the ball screw on the gantry, and the translation in Y axis is achieved by meshing transmission between machine gantry and the

lower half of the machine body. The parallel working head 1 can move in the Z axis and rotate around the X axis and Y axis. 3 DOF of the parallel working head is achieved by stretch of three telescopic rods. Compared with the traditional 5-DOF-serial robot, this new type of hybrid robot has several advantages, such as simple structure, strong carrying capacity, high precision, small inertia, etc. In addition, compared with 5-DOF-serial robot, this hybrid robot has the advantages of quick response speed, small accumulated error and easy implementation. [Jinsong Wang and XinJun Liu, 2002] investigated analysis of a novel cylindrical 3-DOF parallel robot and [Jumpei Arata et al, 2010] studied on a newly developed redundant parallel mechanism.

A hybrid robot with appropriate control strategy can make the tip point achieve good location accuracy in the process of the movement and reduce the error of position control, so as to get better surface machining quality. [Julien Mintenbeck and Ramon Estana, 2010] studied on control of a hyper-redundant 3-RPS parallel mechanism and [Takashi Harada and Motoya Nagase, 2010] studied on impedance control of a redundantly actuated 3-DOF planar parallel link mechanism. Three kinds of control strategies of hybrid robot are studied in the paper, namely PD control algorithm, PD control algorithm with gravity compensation and computed torque algorithm. The purpose is to determine the best control strategy with strong anti-jamming ability so that it will provide the basis for the precise motion control.

Figure 1 Physical model of the new type hybrid engraving Robot

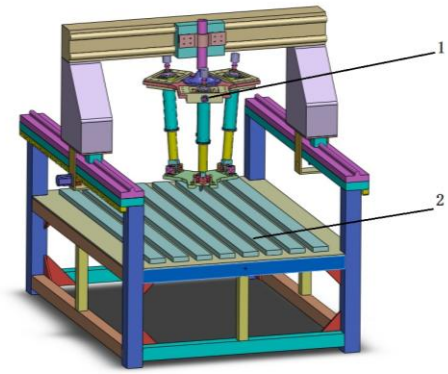

1-the parallel working head;2-the gantry machine body

Figure 2 3-D model of the new type hybrid robot

2 Kinematics analysis of the new type hybrid Robot

Kinematics analysis of the machine body is relatively simple, so the kinematics analysis and control strategy of the parallel working head are studied first.

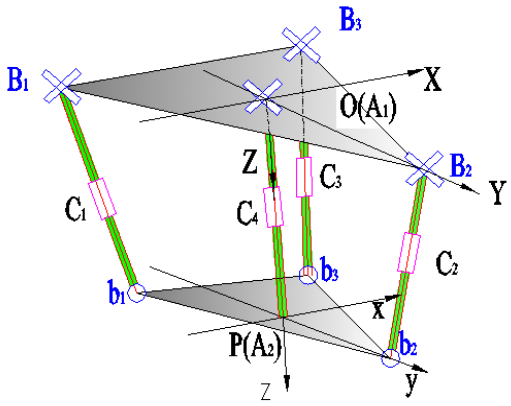

Figure 3 The schematic diagram of parallel working head

The parallel working head of the new type hybrid robot is consisted of the static platform, the moving platform, the telescopic rods and the constraint chain. As shown in figure 3, three telescopic rods are connected by hooke hinges[B_1,B_2,B_3] with the static platform, which are connected by the ball hinges[b_1,b_2,b_3] with the moving platform. Three telescopic rods with slide hinges[C_1,C_2,C_3] are driving rod of the parallel working head. The constraint chain is connected by hooke hinge[A_1] with the static platform, which is connected with slide hinge[C_4] and fixed by the moving platform at the other end.

The inscribed circle radius of the static platform is R_1, Static coordinate origin O coincides with centroid of the static platform. Among them, Y axis is exactly just through the point B_2, Z axis is vertically upwards through the origin O and X axis intersects B_2B_3; The radius of the circumscribed circle of moving platform is R_2. Moving coordinate origin p coincides with centroid of the moving platform. Among them, Y axis is exactly just through the point b_2, z axis is vertically upwards through the origin p and x axis intersects b_1b_2.

In the static coordinates O – XYZ, we can get

$$B_1 = (-\frac{\sqrt{3}}{2}R_1, -\frac{1}{2}R_1, 0),\quad B_2 = (0, R_2, 0),$$

$$B_3 = (\frac{\sqrt{3}}{2}R_1, -\frac{1}{2}R_1, 0), \text{ and } A_1 = (0,0,0).$$

In the moving coordinate p-xyz, we have

$$b_1 = (-\frac{\sqrt{3}}{2}R_2, -\frac{1}{2}R_2, 0),\quad b_2 = (0, R_2, 0)$$

$$b_3 = (\frac{\sqrt{3}}{2}R_2, -\frac{1}{2}R_2, 0), \text{ and } A_2 = (0,0,0).$$

The following equation is established by using coordinate transformation:

$$(X、Y、Z)^T = [T_{op}](x,y,z)^T \quad (1)$$

In the moving coordinate, homogeneous equation of the end of the actuator p relative to the static coordinate is:

$$T_{op}=\begin{bmatrix} c\beta & s\beta s\alpha & s\beta c\alpha & 0 \\ 0 & c\alpha & -s\alpha & 0 \\ -s\beta & c\beta s\alpha & c\beta c\alpha & Z_p \\ 0 & 0 & 0 & 1 \end{bmatrix}$$

Homogeneous coordinates of b_1,b_2,b_3 hinge points on the moving platform in the static coordinates is:

$$\begin{bmatrix} X_{b1} \\ Y_{b1} \\ Z_{b1} \\ 1 \end{bmatrix}=T\begin{bmatrix} -\frac{\sqrt{3}}{2}R_2 \\ -\frac{1}{2}R_2 \\ 0 \\ 1 \end{bmatrix}=\begin{bmatrix} -\frac{1}{2}R_2(\sqrt{3}c\beta+s\alpha s\beta) \\ -\frac{1}{2}R_2c\alpha \\ \frac{1}{2}R_2(-c\beta s\alpha+\sqrt{3}s\beta)+Z_p \\ 1 \end{bmatrix}$$

$$\begin{bmatrix} X_{b2} \\ Y_{b2} \\ Z_{b2} \\ 1 \end{bmatrix}=T\begin{bmatrix} 0 \\ R_2 \\ 0 \\ 1 \end{bmatrix}=\begin{bmatrix} R_2s\beta s\alpha \\ R_2c\alpha \\ R_2c\beta s\alpha+Z_p \\ 1 \end{bmatrix}$$

$$\begin{bmatrix} X_{b3} \\ Y_{b3} \\ Z_{b3} \\ 1 \end{bmatrix}=T\begin{bmatrix} \frac{\sqrt{3}}{2}R_2 \\ -\frac{1}{2}R_2 \\ 0 \\ 1 \end{bmatrix}=\begin{bmatrix} \frac{1}{2}R_2(\sqrt{3}c\beta-s\beta s\alpha) \\ -\frac{1}{2}R_2c\alpha \\ -\frac{1}{2}R_2(c\beta s\alpha+\sqrt{3}s\beta)+Z_p \\ 1 \end{bmatrix}$$

Therefore, length vector L_i of three driving rod can be represented in the static coordinate as follows:

$$B_i=T_{op}b_i \qquad i=1,2,3 \tag{2}$$

$$L_i=B_{Bi}-B_i \qquad i=1,2,3 \tag{3}$$

The length of three telescopic rods is:

$$L_i^2=L_{ix}^2+L_{iy}^2+L_{iz}^2 \qquad i=1,2,3 \tag{4}$$

The kinematics inverse solutions are listed as follows.

$$L_1=\sqrt{(X_{Bi}-X_{bi})^2+(Y_{B1}-Y_{b2})^2+(Z_{Bi}-Z_{bi})^2}$$

$$L_2=\sqrt{(X_{B2}-X_{b2})^2+(Y_{B2}-Y_{b2})^2+(Z_{B2}-Z_{b2})^2}$$

$$L_3=\sqrt{(X_{B3}-X_{b3})^2+(Y_{B3}-Y_{b3})^2+(Z_{B3}-Z_{b3})^2}$$

For the positive solution of the kinematics model, $\alpha,\beta,\mathrm{Z_p}$ can be obtained by using the following analysis method.

$$\alpha=ar\sin\frac{2\sqrt{3}(L_1^2-L_3^2)}{R_1^2R_2^2c\beta s\beta} \tag{5}$$

$$\beta=ar\sin\frac{L_1^2-L_3^2+\sqrt{3}R_2Z_p}{-\sqrt{3R_1R_2s\alpha}} \tag{6}$$

$$Z_p=\sqrt{L_2^2-R_1^2-R_2^2+2R_1R_2c\alpha+R_2^2(c\beta^2)(s\alpha^2)}-R_2c\beta c\alpha \tag{7}$$

The position vector of the tip point in the static coordinate is:

$$\begin{bmatrix} X \\ Y \\ Z \end{bmatrix}=\begin{bmatrix} Z_ps\beta \\ Z_ps\alpha c\beta \\ -Z_pc\alpha c\beta-L_d \end{bmatrix}$$

3 Dynamics analysis of the new type hybrid robot

Based on the Lagrange Functional Equation, the dynamic equation for the moving platform is :

$$M(q)\ddot{q}+V_m(q,\dot{q})\dot{q}+G(q)=\tau \tag{8}$$

where $\tau=J^T\vec{F}$, $M(q)=M_{up}$, $V_m(X,\dot{X})=V_{mup}$, and $G(q)=G_{up}$

The inertia matrix M(X) can be derived from the kinetic energy expression of the moving platform directly. Gravitational coefficient can be given by the following potential energy equation.

$$G(q)=\frac{\partial P_{up}}{\partial X_p}.$$

But the calculation of Coriolis term ($V_m(q,\dot{q})$) is slightly more complicated.

$$M_{up}=\begin{bmatrix} \frac{1.67(0.09-y^2)^2}{\Delta}+50 & \frac{1.67xy(0.09-y^2)}{\Delta} & 0 \\ \frac{1.67xy(0.09-y^2)}{\Delta} & \frac{(0.0405+1.67x^2y^2-0.45x^2-0.45y^2)}{\Delta}+50 & 0 \\ 0 & 0 & 50 \end{bmatrix}$$

where $\Delta=(0.09-y^2)(0.09-x^2-y^2)$.

$$V_{mup}=\begin{bmatrix} V_{11}^u & V_{12}^u & V_{13}^u \\ V_{21}^u & V_{22}^u & V_{23}^u \\ V_{31}^u & V_{32}^u & V_{33}^u \end{bmatrix},$$

which can be deduced by the following formula.,

$$V_m(q,\dot{q})=\frac{1}{2}[\dot{M}(q)+U_M^T-U_M]$$

where
$$\begin{cases} \dot{M}(q)_{kj}=\sum_{i=1}^{3}\frac{\partial m_{kj}(q)}{\partial q_i}\dot{q} \\ U_M^T(q)_{kj}=\sum_{i=1}^{3}\frac{\partial m_{ki}}{\partial q_i}\dot{q}_i \\ U_M(q)_{kj}=\sum_{i=1}^{3}\frac{\partial m_{kj}(q)}{\partial q_k}\dot{q}_i \end{cases}$$

and we have $P_{up} = m_{up} g p_z$, $G_{up} = \dfrac{\partial P_{up}}{\partial X_p}$.

The driving force of the moving platform is:

$$\vec{F}_{up} = (J^T)^{-1}(M_{up}\dot{q} + V_{mup}\dot{q} + G_{up})$$

namely: $\vec{F} = \vec{F}_a + \vec{F}_v + \vec{F}_{gc}$

where $\vec{F}_a$ stands for the end of the acceleration of the actuator caused by the driving force of the moving platform; $\vec{F}_v$ stands for the driving force which overcomes centrifugal force and coriolis force of the moving platform; $\vec{F}_g$ stands for the driving force which overcomes gravity of the moving platform.

Kinematics and Kinetic equations express the relationship between its movement parameters and force suffered by the parallel working head. They are foundations for the further motion control research.

4 Control strategy of hybrid robot

As mentioned above, three kinds of control strategies are adopted in this paper, which are PD algorithm, PD algorithm with gravity compensation and computed torque algorithm, and the best one of them will be used in the new type of hybrid robot.

According to the control strategy, control diagram is proposed to establish the equation of motion control, and on this basis, simulation work and results are investigated.

4.1 PD Algorithm

PD algorithm is simple and has small amount of real-time calculation, which is commonly used in the robot motion control. System control block diagram is shown in figure 4.

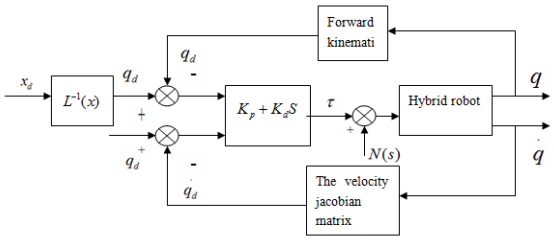

Figure 4 System block diagram for PD algorithm

Where $K_d = diag(K_{d1}, K_{d2}, K_{d3}), K_{di} > 0 (i = 1,2,3)$;

$K_p = diag(K_{p1}, K_{p2}, K_{p3})$ $K_{pi} > 0$ $(i = 1,2,3)$;

In the block diagram, x_d represents the tip point of the desired location; $L^{-1}(x)$ stands for the inverse solution of kinematics equation; N(s) is disturbance; q_d represents the joints of the desired location; q is actual positions of the joint; $\dot{q}_d$ stands for joint expectation speed; $\dot{q}$ represents the actual speed of joints.

The general expression of dynamic equations of hybrid robot joints space is

$$M(q)\ddot{q} + V_m(q,\dot{q})\dot{q} + G(q) = \tau \,, \tag{9}$$

where M(q) stands for the 3×3 inertia matrix; $V_m(q,\dot{q})$ represents a 3×3 coriolis force and centrifugal force vector; G(q) is a 3×1 gravity vector; τ represents the 3×1 control moment vector; q、$\dot{q}$、$\ddot{q}$ stand for the general joint displacement vector, the general velocity vector and the general acceleration vector respectively.

The control law of PD algorithm is

$$\tau = K_p(q_d - q) + K_d(\dot{q}_d - \dot{q}) = K_p e + K_d \dot{e} \tag{10}$$

4.2 PD algorithm with gravity compensation

PD algorithm with gravity compensation is based on the traditional PD algorithm. It considers the factor of gravity compensation. Because the new control strategy considers gravity compensation, the new type hybrid robot under the condition of high speed movement has good control effect. System control block diagram is shown in figure 5.

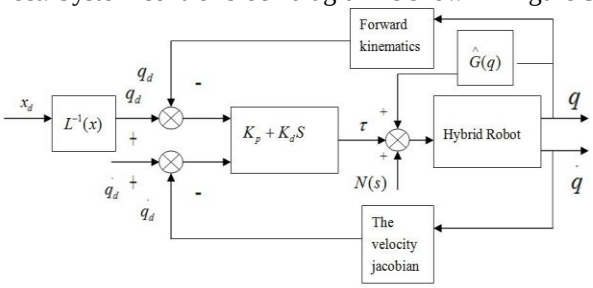

Figure 5 System block diagram for PD algorithm with gravity compensation

The general expression of dynamic equations of hybrid robot joints space is (9).

The control law of PD gravity compensation algorithm is

$$\tau = K_p(q_d - q) + K_d(\dot{q}_d - \dot{q}) + \hat{G(q)} \tag{11}$$

Assuming gravity $G(q)$ can be compensated completely the gravity compensation term $\hat{G}(q)$.

4.3 Computed Torque Algorithm

Computed torque algorithm is based on PD algorithm. It is obtained by adding speed feedback, acceleration feed-forward and gravity compensation in the base of PD algorithm. Figure 6 shows the control system block diagram for computed torque algorithm.

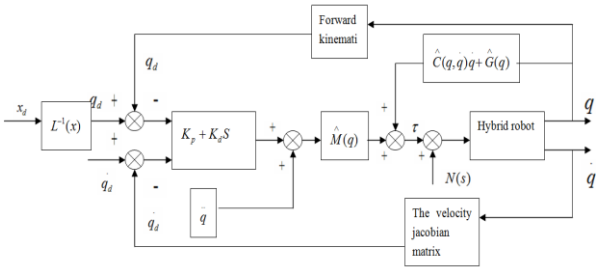

Figure 6 Computed torque algorithm system block diagram

The general expression of dynamic equations of hybrid robot joints space is (9).
Assuming that

$$\hat{M}(q) = M(q), \hat{V}_m(q,\dot{q}) = V(q,\dot{q}), \hat{G}(q) = G(q) \cdot$$

The control law of computed torque algorithm is

$$\tau = M(q)u + V_m(q,\dot{q})\dot{q} + G(q) \tag{12}$$

5 Position control simulation with three kinds of control strategies

In this paper, three kinds of models are used to the simulation work in Matlab/simulink. Simulink is based on the Matlab software package for the dynamic system of modeling and simulation. The package environment provides a number of off-the-shelf modules, which can constitute a dynamic system simulation model through the appropriate link, namely the so-called visual model.
The trajectory model of the parallel working head of hybrid robot is

$$\begin{cases} x = 0.1\sin(\dfrac{2\pi}{T}t) \\ y = 0.1\cos(\dfrac{2\pi}{T}t) \\ z = 0.5 \end{cases}$$

The simulation parameters are listed as follows. The quality of the static platform is 150Kg; the radius of circumscribed circle of the static platform is 0.378m; the quality of the moving platform is 35Kg; the radius of circumscribed circle of the static platform is 0.25m; the quality of each telescopic rod is 25Kg. The simulation time is 7s.

5.1 Simulation for PD algorithm

Parameter settings: $K_d = diag(6000,6000,6000)$, $K_p = diag(2000,2000,2000)$. K_p and K_d are the amplification ratios of P and D in the algorithm.
The minimum value of external random interference signal is 0, the maximum value is 1000.
Then, according to PD algorithm, we got the error curve of moving platform tool tip position and curve of driving force development, which are shown in Figure7.

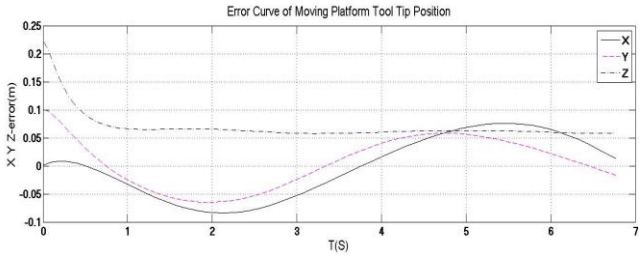

(a)Error curve of moving platform tool tip position

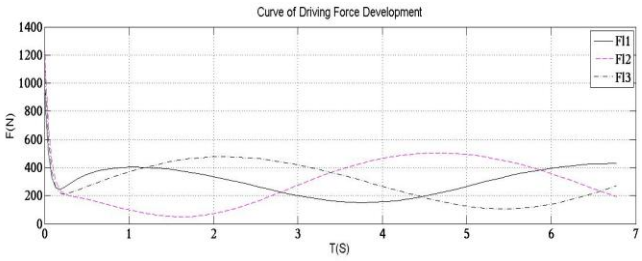

(b)Curve of driving force development

Figure 7 PD algorithm

5.2 Simulation for PD algorithm with gravity compensation

Parameter Settings: $K_d = diag(6000,6000,6000)$, $K_p = diag(2000,2000,2000)$. K_p and K_d are the amplification ratios of P and D in the algorithm.
The minimum value of external random interference signal is 0, the maximum of it is 1000.
Then, according to PD gravity compensation algorithm, we got the error curve of moving platform tool tip position and curve of driving force development, which are shown as Figure 8.

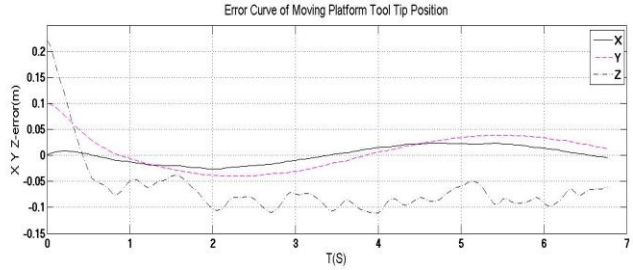

(a)Error curve of moving platform tool tip position

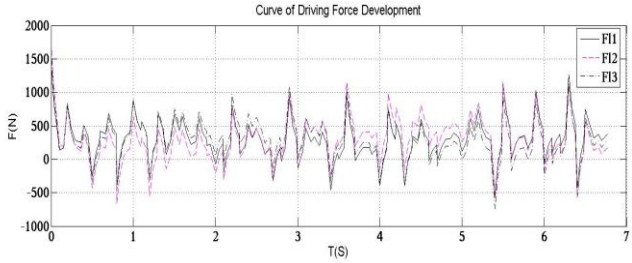

(b)Curve of driving force

Figure 8 PD algorithm with gravity compensation

5.3 Simulation for computed torque algorithm

Parameter Settings: $K_d = diag(6000,6000,6000)$, $K_p = diag(2000,2000,2000)$. K_p and K_d are the amplification ratios of P and D in the algorithm.
The minimum value of external random interference signal is 0, the maximum of it is 1000.
Then, according to computed torque algorithm, we got the error curve of moving platform tool tip position and curve of driving force development, which are shown in Figure 9.

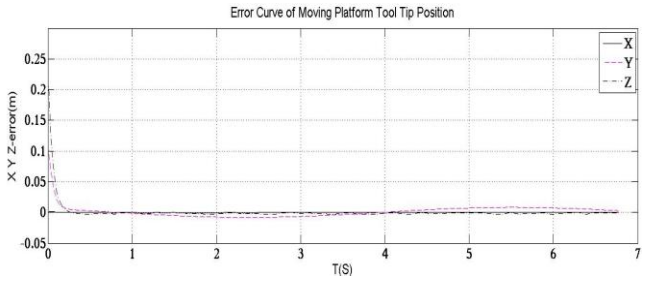

(a)Error curve of moving platform tool tip position

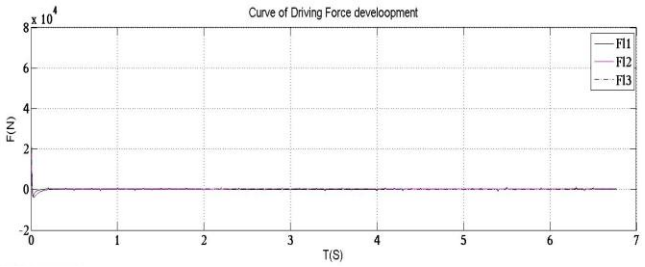

(b)Curve of driving force development

Figure 9 Computed torque algorithm

In Figures 7, 8 and 9, (a) shows relation between error curve of tip point of the moving platform and time in x, y, z directions; and (b) shows relation between force curve of three telescopic rods and time. And we can draw the following two conclusions.

(1)When there is an interference, the tip point positions illustrated by those error curves of the moving platform approach to zero within the simulation time. The ripple of the position error curve of computed torque algorithm is the smallest one among them, and it approaches to zeros with the least time compare with other two control strategies.

(2)When there is an interference, driving forces F_{l1},F_{l2},F_{l3} obtained from PD algorithm varies with time in the simulation period. Driving forces *gained from* PD algorithm with gravity compensation have big jumps over time. However, driving forces obatined from computed torque algorithm approach to zero quickly. It can be seen that computed torque algorithm has strong anti-interference ability.

6 The experiment for computed torque algorithm on the new hybrid type robot

(1)The experimental facilities include the machine body, control system and test system. Control system is composed of NC host, slave unit, motion controller, etc; Test system uses PC computer which is connected with control system through the network cable; Sensors include tension sensor and displacement sensor. Those are shown as in Figure 10 and 11.

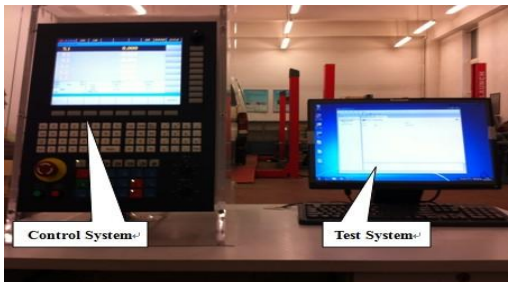

Figure10 Control systems and Test systems

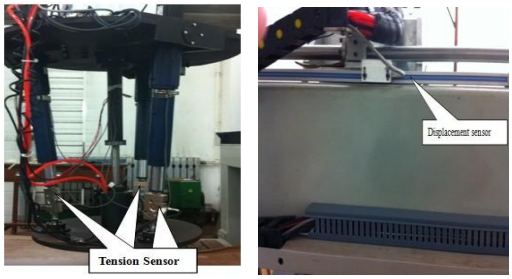

Figure11 Tension Sensor and Displacement Sensor

(2)The experimental process is as follows. Computed torque algorithm is applied as control strategy in the experiment, and horizontal interference force about 1KN is given on the system. Firstly, the motion error of tool tip is tested in experiment. The program is set in control system of the new hybrid type robot, and the velocity of tool tip is 20 mm/s, then the deviations of measuring points are obtained from test system. The error curve of tool tip position is shown in Figure 12; Secondly, Force of three telescopic rods is measured. Because each rod is equipped with tension sensor, the test system can output real-time force curve. The force curve of each rod is shown in Figure 13.

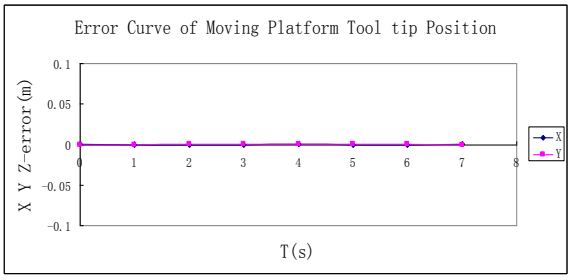

Figure12 Error Curve of Moving Platform Tool Tip Position

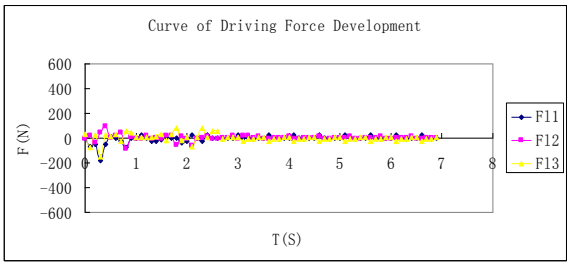

Figure13 Curve of Driving Force Development

(3) The experimental results

Comparing Figure 9 with Figure 12 and Figure 13, it is observed that simulated curves and experimental line graphs are similar in their trend. The experiments of motion error show that the maximum displacement deviation is 0.68mm, and the error range is from -0.68mm to 0.4mm. The force test data evidence that the range of force change is from -180.97N to 92.77N, and the system comes back to normal within 0.8 seconds.

When changing the value of horizontal interference force to 1.5KN, 2KN and 2.5KN, the above experiment is repeated. Their curves of driving force development are similar in the trend, which come back to normal within 0.8 seconds, so it indicates the system is robust.

Experimental results indicate that control precision of computed torque algorithm for the new hybrid type robot is high and achieve the ideal control effect.

7 Conclusions

The motion control strategy of the new type hybrid engraving robot is studied in the paper. Based on kinematics analysis, three kinds of control strategies, PD algorithm, PD algorithm with gravity compensation and computed torque algorithm are presented to build the control models. All control strategies are simulated by Matlab\Simulink software, and the advantages and disadvantages of different control strategies are compared. The results show that position control effect of computed torque algorithm is the best one among these three kinds of control strategies and the corresponding system has strong anti-jamming ability. In the case of applying multiple sets of horizontal interference force, control system with computed torque algorithm can quickly restore stability, hence it shows the system has a certain robustness. Therefore, computed torque control algorithm can be used in the new type hybrid engraving robot.

References

[Bruno Monsarrat et al, 2003] Bruno Monsarrat and Clément M. Gosselin, Workspace analysis and optimal design of a 3-Leg 6-DOF parallel platform mechanism, *IEEE Trasaction on Robotics and Automation*,,19(6): 954-966, 2003.

[Binbin Peng et al, 2010] Binbin Peng, Zengming Li, Liangbin Zeng and Yu Sun, A novel high speed 2-DOF translational parallel robot for pick-and-place operations, *2010 International Conference on Computer, Mechatronics, Control and Electronic Engineering*, pages 522-525, Nanjing, China,2010.

[Chi Hyo Kim et al, 2007] Chi Hyo Kim, Sung Joo Kim, Kun Woo Park and Jin Ho Kyung, Topological design of the 5-DOF parallel-wrist manipulator with a constraining mechanism. *International Conference on Control, Automation and Systems 2007*, pages 2278-2282, COEX, Seoul, Korea, Oct.17-20, 2007.

[Fabrizio Patanè and Paolo Cappa, 2011] Fabrizio Patanè and Paolo Cappa, A 3-DOF parallel robot with spherical motion for the rehabilitation and evaluation of balance performance. *IEEE Transactions on Neural Systems and Rehabilitation Engineering*, 19(2),:157-166, 2011.

[Jinsong Wang and XinJun Liu, 2002] Jinsong Wang, and XinJun Liu,Analysis of a novel cylindrical 3-DoF parallel robot, *Robotics and Autonomous Systems*, 42, 31-46, 2003.

[Joon Woo Kim et al, 2007] Joon Woo Kim, Kun Woo Kim, Han Sung Kim and Jin Ho Kyung. Stiffness analysis and design of a 3-DOF parallel robot with one constraining leg. *International Conference on Control, Automation and Systems*, pages 2288-2293, COEX, Seoul, Korea, Oct. 17-20, 2007.

[Jumpei Arata et al, 2010] Jumpei Arata, Hiroyuki Kondo, Norio Ikedo, and Hideo Fujimoto, Haptic device using a newly developed redundant parallel mechanism, *IEEE Transactions on Robotics*, 27(2):201-214, April 2011.

[Julien Mintenbeck and Ramon Estana, 2010] Julien Mintenbeck and Ramon Estana, design, modelling, control of a hyper-redundant 3-RPS parallel mechanism. *proceedings of the 2010 IEEE international conference on robotics and biomimetics*, pages 591-596, Tianjin, China, December 14-18, 2010.

[Nicolas Lauzier and Clement Gosselin, 2010] Nicolas Lauzier and Clement Gosselin, 3-DOF cartesian force limiting device based on the delta architecture for safe physical human-robot interaction. *2010 IEEE International Conference on Robotics and Automation*, pages 3420-3425, Anchorage, Alaska, USA, May 3-8, 2010,

[Takashi Harada and Motoya Nagase, 2010] Takashi Harada and Motoya Nagase, Impedance control of a redundantly actuated 3-DOF planar parallel link mechanism using direct drive linear motors. *Proceedings of the 2010 IEEE International Conference on Robotics and Biomimetics*, pages 501-506, Tianjin, China, December 14-18, 2010.